coatings

MDPI

Article

Effect of Composite Fibers and Fly Ash on the Properties of Portland–Sulfoaluminate Composite Cement-Based Grouting Sealing Materials

Jiming Bao [1], Xuzheng Zhu [2,*], Shanyang Wei [2], Feng Ren [1], Weidong Luo [3] and Shuqi Xu [2]

[1] Guizhou Zisenyuan Group Investment Co., Ltd., Liupanshui 550034, China
[2] Mining College, Guizhou University, Guiyang 550025, China
[3] Guizhou Panjiang Coal Power Group Technology Research Institute Co., Ltd., Guiyang 550025, China; lwlf925929@163.com
* Correspondence: 18851906030@163.com

Abstract: Current conventional cement materials are no longer able to meet the actual usage needs of geotechnical engineering. In order to improve the workability of cement materials used in geotechnical, transportation, and mining engineering, it is necessary to improve the formulation of cement materials. Polypropylene fibers (PVAF), polyvinyl alcohol fibers (PPF), and fly ash (FA) are used in this study to modify Portland–sulfoaluminate composite cement to improve the workability of the cement material system. Meanwhile, the microstructure that affects the system performance was also studied. The research results indicate that adding FA to the composite cement system can improve its fluidity. In the later stage of hydration, due to the volcanic ash reaction, the production of hydration products will increase, but it will not affect the type of hydration products. Adding PPF-PVAF can effectively improve the strength performance of the cement system. The compressive strength reached 24.61 MPa after 28 days of curing, which was 13.8% higher than the blank sample. Adding calcium hydroxide powder and FA to the system can improve the fluidity of the cement system to a certain extent and positively impact the later strength. After 28 days of curing, the compressive strength of experimental group 9 reached 30.21 MPa, which increased by 70.5% compared to after 7 days These results were found at the microscopic level, based on analyses via XRD, TG, and SEM. The Mix-EXP cured for 28 days has better hydration product content and composition arrangement of cement slurry than the O-S-C cured for 28 days.

Keywords: cement-based material; cement performance; fly ash; fiber additives; microstructure

Citation: Bao, J.; Zhu, X.; Wei, S.; Ren, F.; Luo, W.; Xu, S. Effect of Composite Fibers and Fly Ash on the Properties of Portland–Sulfoaluminate Composite Cement-Based Grouting Sealing Materials. *Coatings* **2024**, *14*, 989. https://doi.org/10.3390/coatings14080989

Academic Editor: Andrea Nobili

Received: 24 June 2024
Revised: 24 July 2024
Accepted: 1 August 2024
Published: 6 August 2024

1. Introduction

With the advancement of development projects in western China, underground projects such as tunnel construction and mining development are gradually moving towards tunnel construction and mining development in the central and western regions. The more complex geological environment and the increasing difficulty of geological disaster prevention and control have put forward new requirements for engineering technology and material properties.

Grouting technology is widely used in tunnel construction, mining, and geotechnical engineering to prevent water inrush, reinforce broken surrounding rocks, etc. [1–4]. The sulfoaluminate cement (SAC) invented by Chinese researchers in the 1960s has the characteristics of high early strength, corrosion resistance, and shrinkage compensation [5–7], which was initially promoted and used as a material to compensate for the shrinkage performance of ordinary Portland cement (OPC). Now, it has been actively used as a common grouting material in various construction sites [8–10]. At present, SAC is gradually exposed to problems such as difficulties in controlling the setting time and a decrease in the strength of cement in the middle and later stages, which limits its stability in engineering

applications. In underground engineering, such as tunnels and geotechnical engineering, the later strength reduction in grouting materials will lead to problems such as faults, tunnel leakage, and reduced efficiency of mine gas extraction, seriously affecting the project quality [11,12]. In addition, with the proposal of the "dual carbon" theory, in the context of carbon peaking and carbon neutrality, according to the initiatives of relevant departments and industry associations, China's construction materials industry is expected to fully achieve carbon peaking by 2025, including the cement industry [13,14].

In recent years, to improve the issues above, many researchers have attempted to improve the performance of the sulfoaluminate cement system by adding fibers, limestone powder, and other substances as well as by partially replacing cement with fly ash (FA) to reduce carbon emission faults [15–17].

In the production process of Portland cement clinker, the use of limestone will emit a large amount of CO_2, while the calcination temperature of SAC lowers by 100–150 °C compared to Portland cement, which can reduce energy consumption by 27% to 37% and, correspondingly, reduce CO_2 emissions by 18% to 48% [18]. Therefore, the appropriate application of SAC can reduce CO_2 emissions in the production process and positively affect overall sustainable development.

SAC has specific expansion characteristics, and the degree of expansion can be controlled by adding Portland cement to the sulphoaluminate cement system [19]. The mixture of sulfoaluminate cement and Portland cement (OPC–SAC mixture) is also known as type-K cement [20]. According to the relevant research, adding 10% SAC to the Portland cement system does not affect the hydration mechanism of tricalcium silicate. However, the increase in sulfate content in the system will delay the tricalcium silicate reaction and, to some extent, increase the amount of ettringite [21]. The increase in ettringite content will shorten the overall early hardening time of the composite cementitious system and enhance the early strength of the system.

Fly ash (FA) mainly comes from the solid waste generated by coal-fired power generation in thermal power plants and is a potentially valuable artificial volcanic ash resource [22–24]. Scholars have found that the rational use of high-quality FA in concrete can benefit concrete systems. At present, a large number of experts and scholars have incorporated FA into cement-based materials to improve the relevant properties of cement-based materials, achieving the goals of reducing costs, improving workability, and increasing strength and durability [25,26]. When fly ash is present in the system, adding calcium hydroxide can significantly shorten the setting time of the composite cement slurry. When mixed with FA, it can improve the compressive strength of the cementitious material in the composite cement–fly ash system. Moreover, with the increase in calcium hydroxide content, the strength of the composite material gradually increases. In alkaline environments, the hydration process of cement will accelerate, with an increase in the amount of ettringite in the early stages of hydration. Additionally, calcium hydroxide can react with aluminum silicate glass in fly ash to generate more C-S-H cementitious materials, fill harmful pores in hardened cement paste, and improve the structure of cement paste [27,28].

Polyvinyl alcohol fiber (PVAF) material has a strain-hardening effect and high ultimate tensile strain [29–32]. Adding fibers to cement can improve the early mechanical properties of the cement matrix but may, to some extent, weaken the compressive strength of a 28-day-old cement matrix [33]. Some scholars have also studied the influence of fiber length on the dispersion amounts of fibers in the medium system with fibers added. Their studies found that fiber length affects the dispersion amounts of fibers in the medium system. The longer the fiber, the smaller its dispersion amount in the dispersion medium is and the easier it is to aggregate, resulting in a decrease in the fluidity of the slurry [34]. Another type of fiber, polypropylene fiber (PPF), has the characteristics of high strength, high toughness, stable chemical properties, chemical corrosion resistance, and easy uniform dispersion in cement concrete systems [35,36].

The main objective of this study is to combine OPC with SAC and add materials such as FA, PPF, and PVAF to the composite cement system to improve the compressive,

flowability, and setting properties of cement materials. At the same time, micro testing and analysis methods are used to explore the reasons for the differences between the mixed cement system and ordinary cement.

2. Experimental Study

2.1. Raw Materials

This study used 42.5 grade OPC and low-alkalinity SAC, with fly ash (FA) added as the substrate. The PPF (polypropylene fiber) and PVAF (polyvinyl alcohol fiber) used as additives come from Shanghai Chenqi Chemical Technology Co., Ltd., Nanqiao Town, China, and the calcium hydroxide comes from Xilong Chemical Co., Ltd., Shantou, China. The chemical composition of SAC, OPC, and FA is shown in Table 1, and the performance parameters of cement and fibers used in the experiment are shown in Tables 2 and 3.

Table 1. Chemical composition of OPC, SAC, and FA.

Components	SiO_2	Al_2O_3	Fe_2O_3	CaO	MgO	SO_3	Na_2O	TiO_2	Loi
OPC/wt.%	18.81	4.71	2.71	60.21	2.21	3.55	0.732	0.63	3.78
SAC/wt.%	7.1	17.83	4.11	3.71	0.49	18.81	0.86	1.49	2.21
FA/wt.%	57.4	28.6	3.86	1.44	2.71	0.45	3.66	-	0.33

Table 2. Physical properties of cements.

	W/C	Setting time/min		Compressive strength/MPa		Flexural strength/MPa	
OPC		Initial	Final	3 d	28 d	3 d	28 d
	0.5	213	280	14.5	45.8	6.0	8.9
	W/C	Setting time/min		Compressive strength /MPa		Flexural strength /MPa	
SAC		Initial	Final	1 d	7 d	Initial	Final
	0.5	25	36	10.6	50.4	6.4	7.9

Table 3. Physical properties of PPF and PVAF.

Product Name	Diameter/μm	Fiber Length/mm	Tensile Strength/MPa	Elastic Modulus/GPa
PPF	48	6	450	8
PVAF	20	6	1600	35

2.2. Sample Mix Proportion Plan and Specimen Production

The water–cement ratio used in this experiment was 0.5, and the blank control group was made of an OPC–SAC mixture. FA at 10% and 20% was used to replace cement to make cement mortar. In addition, experimental groups with different fiber dosages were set up based on the blank group. The experimental plan is shown in Table 4. The production steps of the specimen are as follows: First, weigh the cement, FA, and water reducer and pour them into a mixer. Stir at low speed (140 ± 5 r/min) for one and a half minutes, mix evenly, add sufficient tap water, continue stirring at low speed for 90 s, and mix at high speed (285 ± 10 r/min) for 90 s. Finally, pour the evenly mixed cement mortar into a 70 mm × 70 mm × 70 mm cement test mold and place it in a curing box. Set the temperature to 20 ± 2 °C and humidity to 90 ± 5% for the corresponding curing time. After reaching the expected curing time (1 d, 7 d, 14 d, and 28 d), take it out for testing. The preparation process of cement samples is shown in Figure 1.

Table 4. Cement mix proportion of specimens.

Experiment Group Number	Specimen Code	Weight/g					
		OPC	SAC	FA	PPF	PVAF	Water
1	O-S-C(control)	700	300	0	0	0	500
2	O-S-FA0.1	630	270	100	0	0	500
3	O-S-FA0.2	560	240	200	0	0	500
4	O-S-PPF1.0	700	300	0	1.0	0	500
5	O-S-PPF2.0	700	300	0	2.0	0	500
6	O-S-PVAF1.0	700	300	0	0	1.0	500
7	O-S-PVAF2.0	700	300	0	0	2.0	500
8	O-S-PP&PVA	700	300	0	1.5	0.5	500
9	Mix-EXP	630	270	100	1.5	0.5	500

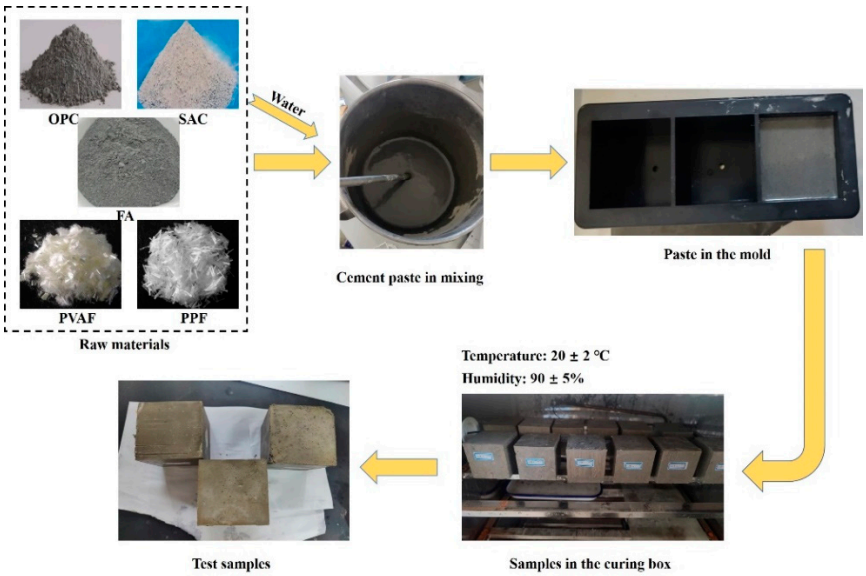

Figure 1. Cement sample preparation process.

2.3. Test Methods

2.3.1. Setting Time and Fluidity

According to the requirements of GB/T1346-2011 (ISO 9597:2008), the setting time of the cement mortar material prepared in this experiment was measured using a Vicat apparatus [37]. Before measuring the setting time, it is necessary to check whether the movement of the metal rod is restricted and adjust the test needle of the zeroing caliper. Inject the cement slurry into the test mold, shake and scrape it flat, and cure it. The initial time for measuring the setting time is the time when water is added to the cement and stirred. The main steps of the setting time test are as follows: after counting for 30 min, take the specimen out of the curing box for the first test. Install the initial setting test needle, place the test piece horizontally under the test needle, adjust the needle tip of the initial setting test needle to just touch the surface of the test piece, tighten the screw, wait for 1–2 s to quickly relax the test piece, let the test needle fall freely into the test piece, and read the scale after the test needle stops sinking or is released for 30 s. When the test needle sinks to a distance of 4 mm ± 1 mm from the glass plate and no longer changes, the specimen reaches the initial setting state. The time from the start of stirring is the initial setting time of the specimen. After measuring the initial setting time, replace the final setting test needle and flip the mold 180° onto the glass plate to continue curing. Conduct a test every 15 min, and be careful not to let the test needle repeatedly fall into the pinhole left by the previous test. When the final setting test needle sinks to the surface of the specimen by 0.5 mm or no longer leaves any circular marks, the specimen reaches the final setting state.

The fluidity test of cement slurry was conducted in accordance with the relevant requirements of the "Method for Determining the Fluidity of Cement Mortar" (GB/T2419-2005) [38]. The main experimental steps are as follows: before testing, wipe the mold, glass plate, and other testing tools with a wet towel to keep them moist, place the truncated cone round mold in the center of the glass plate, and prepare the cement slurry according to the standard. Quickly inject the prepared cement slurry into the truncated cone mold and compact it with a scraper to level the surface. Lift the truncated cone mold vertically to allow the cement slurry to flow freely on the glass plate. When the cement slurry begins to flow, use a stopwatch to time it. After the slurry flows for 30 s, use a ruler to measure the maximum diameter in two perpendicular directions and calculate the average value. Each test is conducted three times, and the arithmetic average value is taken as the fluidity test value of the cement slurry.

2.3.2. Mechanical Strength Testing

After curing the specimens in a standard curing box for 1 day, 7 days, 14 days, and 28 days, according to GB/T17671-2021, the YAW-300A microcomputer-controlled electro-hydraulic servo pressure testing machine was selected to test the compressive strength of the experimental specimens, and the sample size was set at 70 mm × 70 mm × 70 mm [39]. The maximum test load was set to 300 KN, and the loading rate was fixed at 1 mm/s. Three specimens were tested in each group to ensure the authenticity of the data.

2.3.3. X-ray Diffraction Analysis

X-ray diffraction is a widely used and validated crystallographic analysis method. X-ray has a short wavelength and strong penetration ability, which can analyze materials based on their composition and composition. Crystal materials are generally composed of crystal cells with regular atomic arrangement. X-ray diffraction can be used to analyze the phase and crystal structure of crystal materials. Perform X-ray diffraction analysis on the specimen and analyze the products of cement hydration reaction through Cu Ka radiation, with the radiation range set to 2θ (5–70°) [40,41]. After the specimen reaches the curing age, soak the raw material sample in anhydrous ethanol for one week, terminate the hydration reaction of the sample, and prepare the powder for scanning. When preparing the sample powder, an appropriate amount of anhydrous ethanol can be added for wet grinding and placed in an oven to dry at 40 °C for 48 h. After drying, use the instrument to scan the sample powder.

2.3.4. Thermogravimetric Analysis

Thermogravimetric analysis is a method of measuring the relationship between material mass, temperature, and time by controlling temperature through a program. By heating the test sample at high temperature and recording the mass loss in the sample, it is possible to study the composition of the material and its possible products and further obtain the thermal stability of the sample as well as the relationship between the composition of the sample and the pyrolysis quality [42,43]. The sample preparation process for thermogravimetric analysis is similar to that of X-RD (X-ray diffraction) samples. The analysis steps are as follows: N_2 is used as the protective gas during the analysis process, and 5–20 mg of the sample is placed in an empty crucible until the substance stabilizes and is weighed. The experimental heating temperature range is set to 25–700 °C, and the heating speed is set to 10 °C/min.

2.3.5. Scanning Electron Microscopy

At present, scanning electron microscopy (SEM) analysis is widely used in the study of cement materials. By observing cement samples using SEM, the microstructure, product morphology, and material distribution of cement specimens can be analyzed. At the same time, other methods such as X-ray diffraction or infrared spectroscopy can also be used to qualitatively analyze the hydration reaction rate of samples. This experiment used a field

emission scanning electron microscope to observe multiple sets of cement slurries designed for the experiment and compare the micromorphology and microstructure of the materials. Terminate the hydration reaction of cement samples cured to a certain age using anhydrous ethanol, and then, dry them in a 40 °C oven for 7 days. Finally, fix the samples on a reagent kit and observe the microstructure of the samples after vacuum plating using a scanning electron microscope.

2.3.6. Data Statistical Methods

In this study, each group of experiments was designed with three further subgroups. After conducting three subgroups of experiments, the average of the three groups of experimental data was taken as the final written experimental data for presentation.

3. Results and Discussion

3.1. Setting Time and Fluidity

The statistical charts of coagulation time for different experimental groups are shown in Figure 2. The effect of FA addition on the setting time of cement tends to be consistent, and as the FA content increases, the setting time of the slurry gradually increases. Comparing the O-S-C and O-S-FA0.2 in the figure, it can be found that the initial setting time of the O-S-FA0.2 added with 20% fly ash increased by 298.1% from 55 min to 164 min compared to O-S-C. The final setting time increased from 84 min to 181 min, an increase of 215.5%. However, the setting time of samples mixed with PPF and PVAF did not show significant changes, indicating that the addition of fly ash slowed down the reaction rate in the initial stage of the hydration reaction, ultimately leading to an extension of macroscopic setting time, which consistent with Tehsien Wu's research findings [44].

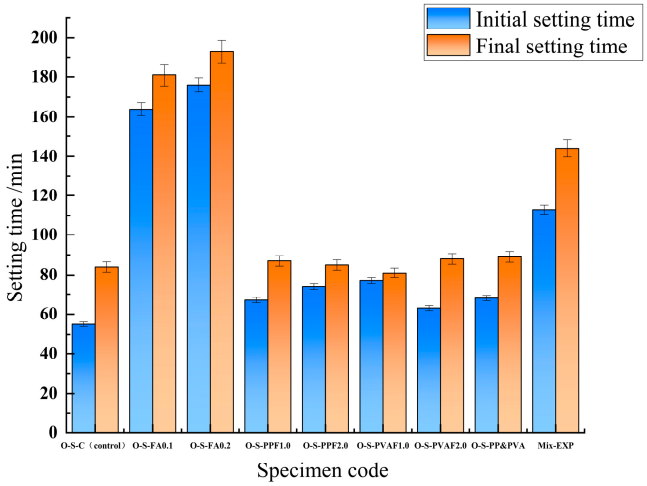

Figure 2. Setting time of cement.

The flowability test data of each experimental group are shown in Figure 3. From the data in the figure, it can be seen that the addition of FA will slightly improve the flowability of the composite cement system. This is because the spherical particles in fly ash have a lubricating effect, reducing the bonding force between particles in the concrete system and increasing the flowability of the system [45,46]. The addition of PPF and PVAF fibers has no significant effect on the flow rate. Due to the addition of a water reducer, the flowability of the experimental group has been effectively improved. However, excessive flowability can decrease viscosity, which may result in poor slurry distribution during hole sealing. Therefore, comprehensive consideration is needed in practical applications.

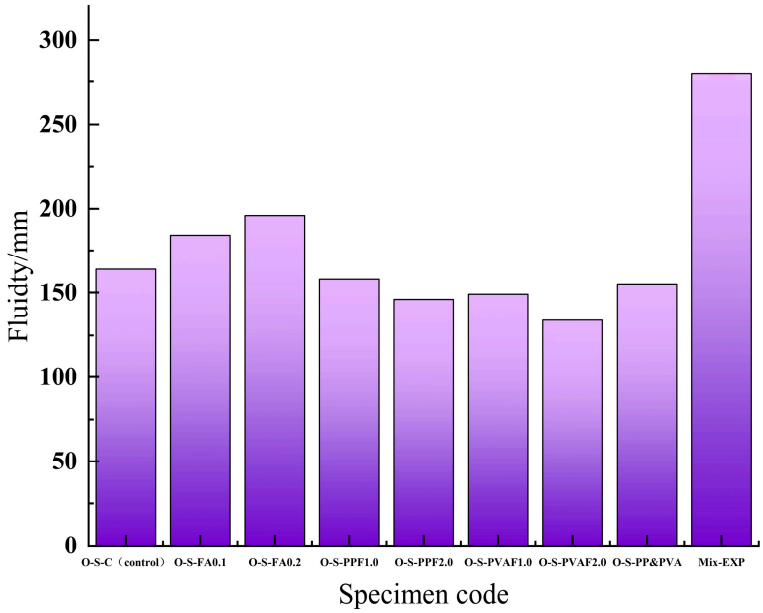

Figure 3. Fluidity of cement slurry.

3.2. Compressive Strength

Select the blank control group of composite cement, the control group with only added fibers, and the experimental group to determine the average compressive strength at different curing ages, as shown in the control bar chart in Figure 4. The graph shows that after 1 day of curing, the compressive strength of the control group added with PVAF was slightly higher than that of the blank group, while the compressive strength of the experimental group was lower. This may be due to the addition of fly ash in the experimental group delaying the hydration reaction of the cement system, resulting in a lack of significant strength improvement in the early stage. After 7 days of curing, the strength of the experimental group reached over 15 MPa, significantly higher than the blank control group and better than the two groups of samples with only added fibers. At 28 days after the hydration reaction, the strength of the experimental group reached 30.21 MPa (±3%~5%), an increase of 39.8% compared to the blank group. This may be because the fiber bonded with the cement system after being mixed into the cement and being closely combined with the matrix, which improves the strength of the cement system. At the same time, the pozzolanic reaction of the fly ash promotes the hydration of the cement system, generating more hydration products such as ettringite, silica hydrogel, calcium sulphoaluminate, etc. [45,46]. These hydration products attach to the surface of PVAF, further improving the cement system's strength.

3.3. Cement Material Post-Treatment

According to the relevant research, adding polycarboxylate superplasticizers to the cement system can improve the properties of cement, such as solidification, flow, and compressive strength [47–49].

Figures 5–7 show the experimental data on the effects of different dosages of water-reducing agents on the flowability, setting time, and compressive strength of cement systems. From the experimental data, it can be seen that the flowability of cement slurry has been improved to some extent after adding water-reducing agents, and the addition of water-reducing agents has a retarding effect on the cement system.

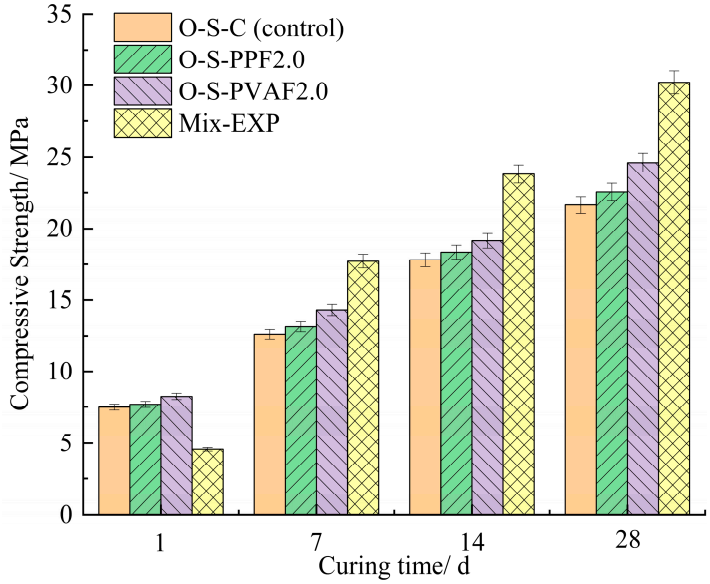

Figure 4. Compressive strength of cement specimens at different curing ages.

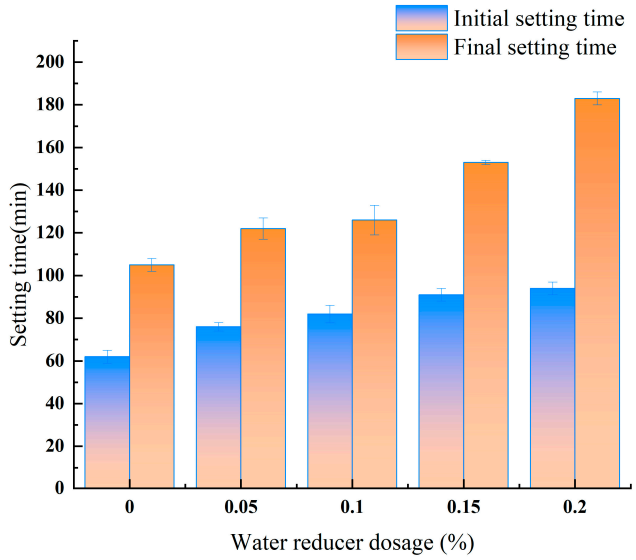

Figure 5. Setting time of O-S-C with different dosages of water reducer.

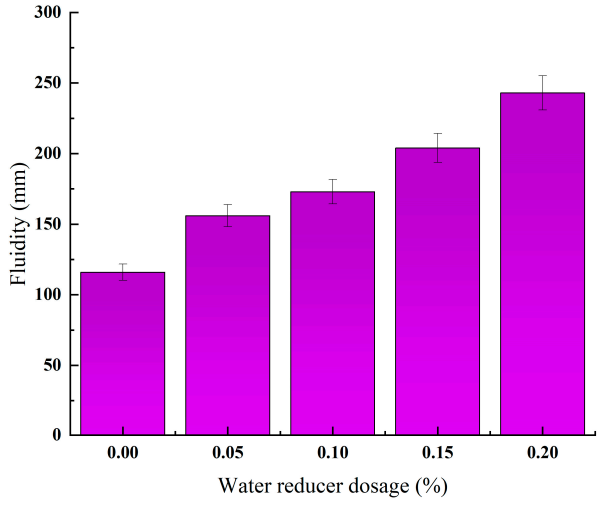

Figure 6. Fluidity of O-S-C with different dosages of water reducer.

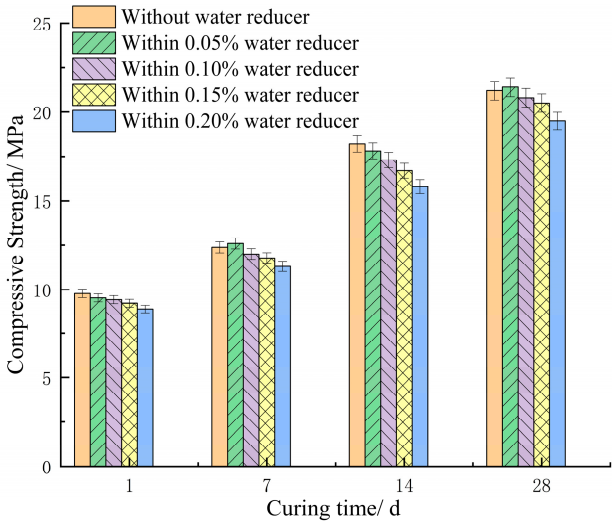

Figure 7. Compressive strength of O-S-C with different dosages of water reducer.

On the basis of the research in the previous section, this section added a water reducer equivalent to 0.2% of the total weight of cement to each group of materials. The setting time, fluidity, and compressive strength data of the experimental group post-treatment are shown in Figures 8–10.

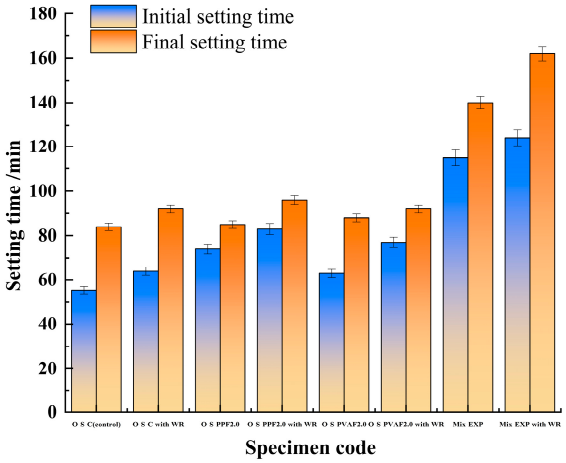

Figure 8. Setting time comparison of cement slurry.

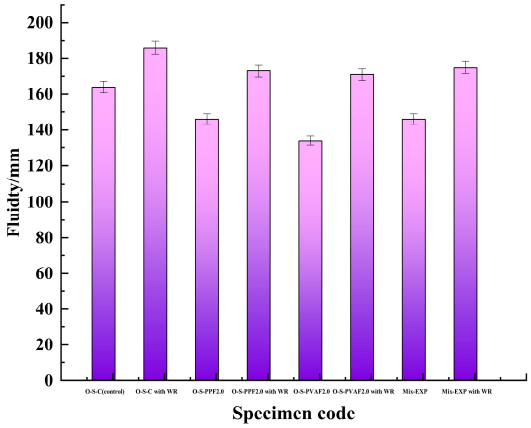

Figure 9. Fluidity comparison of cement slurry.

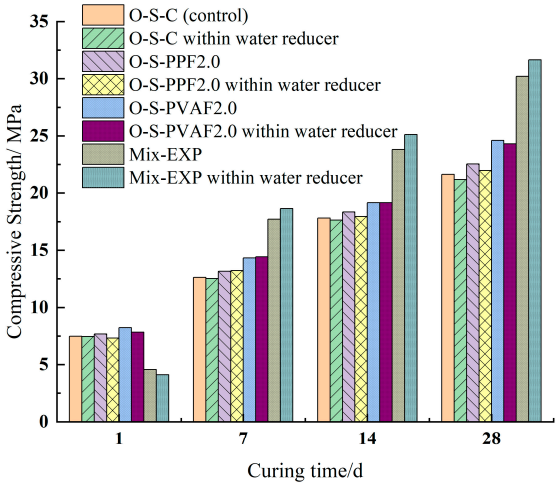

Figure 10. Compressive strength comparison of cement specimens at different curing ages.

Based on the experimental data from Figures 8–10, it can be observed that after adding the water reducer, the setting time of several cement groups was slightly delayed, at about 10–20 min. When the setting time is prolonged, the early hydration of the cement system is hindered by the water reducer, resulting in a slight decrease in the early (1 d, 7 d) strength of several groups of cement. However, adding water reducer to the cement system can reduce the flocculation effect during the cement hydration reaction, making the distribution of hydration products more uniform. Therefore, in the later stage of hydration (28 d), the compressive strength of cement is improved by about 1–2 MPa.

3.4. X-ray Diffraction Analysis

Historical studies have shown that the addition of PPF and PVAF fibers does not significantly impact the hydration of the composite cement system [50]. In order to investigate the effects of other additives in the experimental group on the hydration products, X-ray diffraction (XRD) technology was used to characterize the solidified slurry of the early (1 d) and mid to late (28 d) cement mixtures in this experiment. The X-ray diffraction results of the O-S-C sample and the Mix-EXP sample are shown in Figure 11. From the 1-day hydration reaction graph, it can be seen that the hydration products of the O-S-C and the Mix-EXP are basically the same, but there is a specific difference in hydration progress. This indicates that the added fly ash and calcium hydroxide are not directly involved in the hydration reaction. However, due to the addition of fly ash delaying the early hydration process of the cement system, the O-S-C is at 9° (2θ). The diffraction peak intensity of left and right ettringite is slightly higher than that of the Mix-EXP. As the hydration reaction progresses, the diffraction peak intensity of the main hydration products in the Mix-EXP, such as calcium sulfoaluminate and ettringite, is significantly higher than that of the O-S-C at 28 days, indicating that adding calcium hydroxide to the system can activate fly ash and induce the cement system to accelerate the hydration reaction. At 30° (2θ), the difference in diffraction peak intensity of left and right calcium carbonate also indicates that the calcium hydroxide fly ash activation system can improve the carbon fixation effect of the cement system. Based on the comprehensive X-ray diffraction analysis data, we can find that the aggregate effect of fly ash and the dispersion effect of water-reducing agents effectively promote the hydration process of the cement system.

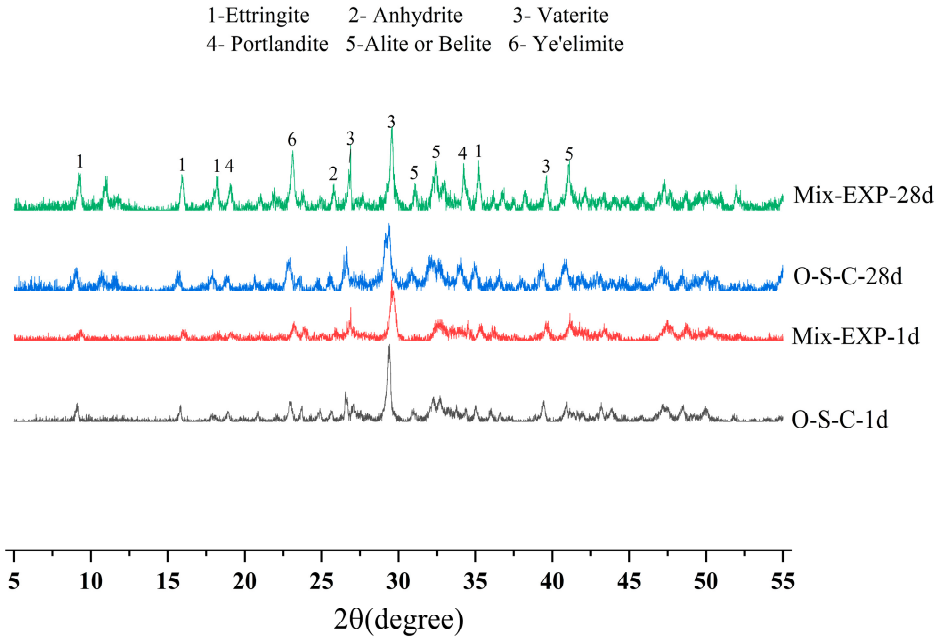

Figure 11. X-RD patterns of hydrated cement pastes at different curing ages.

3.5. Thermal Gravimetric Analysis

The curves shown in Figure 12 are the thermogravimetric analysis curves of cement samples from the O-S-C sample and Mix-EXP sample, with curing ages of 1 day and 28 days. According to the thermogravimetric curve in the figure, the process of mass loss in the thermogravimetric test can be divided into five stages: (1) starting temperature ~170 °C: the loss in free water contained in the silica hydrogel and the loss in bound water in some ettringite; (2) 170~430 °C: further loss in bound water during dehydration of silica hydrogel; (3) 430~475 °C: decomposition of calcium hydroxide crystals; (4) 475~700 °C: loss in bound water during the decomposition of silica hydrogel; (5) temperature greater than 700 °C: the dissociation temperature of calcium carbonate is 705 °C, so after further heating, calcium carbonate will decompose and other hydrates will also be dehydrated; however, due to objective differences in equipment sensitivity, experimental operations, and sample preparation, there may be slight fluctuations in temperature at each stage.

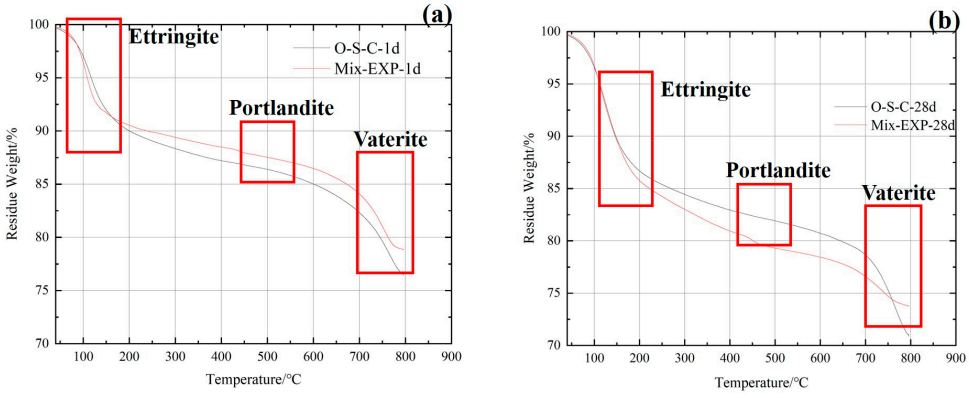

Figure 12. TG patterns of cement pastes at different curing ages (**a**) 1 d; (**b**) 28 d.

It can be seen from the curve in the figure that the hydration products of the Mix-EXP and the O-S-C are basically the same, mainly including C-S-H gel, ettringite, calcium hydroxide, and calcium carbonate formed by carbonization of calcium hydroxide. In terms of the production of hydration products, the curve of the 1-day-old Mix-EXP was higher than that of O-S-C. In contrast, the production of calcium hydroxide and calcium

carbonate in Mix-EXP was lower than in O-S-C. This is because adding fly ash delayed the early hydration reaction of the cement system [51,52]. At the curing age of 28 days, the production of ettringite, calcium hydroxide, and calcium carbonate in Mix-EXP was significantly higher than in O-S-C. The mass loss data in each stage are shown in Table 5. From the data in the table, it can be seen that when the curing age is 1 day, the Mix-EXP has a lower production of ettringite than O-S-C due to the delayed early hydration caused by the addition of fly ash. When the maintenance period reached 28 days, compared to the benchmark group during the same period, the Mix-EXP showed a 6% increase in ettringite production and a 95.91% increase in calcium hydroxide production. In the heating temperature range of 600–750, the loss in mass of this part of O-S-C was higher than that of Mix-EXP. This is because the free water in the system and the bound water around the product were also lost on ignition. During the same curing period, the hydration degree of M ix-EXP was higher than that of O-S-C, consuming most of the free water and bound water present in the system. This also indicates that the pozzolanic reaction of fly ash can promote the production of hydration products to a certain extent, but it can also locally affect the early strength and other properties of the cement system, which is consistent with the previous X-ray diffraction analysis results.

Table 5. Mass changes obtained via thermal gravimetric analysis.

Specimen Code	Mass Loss/%		
	30–170 °C	**430–475 °C**	**600–750 °C**
O-S-C-1 d	9.13	0.39	5.38
Mix-EXP-1 d	8.90	0.47	5.42
O-S-C-28 d	11.73	0.49	5.43
Mix-EXP-28 d	12.43	0.96	3.67

3.6. Microstructure Analysis

Comparing the scanning electron microscopy images of O-S-C and Mix-EXP with a hydration age of 1 day, it can be seen that O-S-C at this time contains a blockier distribution of ettringite and calcium hydroxide compared to Mix-EXP. Although ettringite is produced in the Mix-EXP, its distribution is relatively scattered, and the structure is not dense. This may be due to the dispersion effect of fly ash and water reducer added in the Mix-EXP, resulting in a less concentrated distribution of products in the early stage of cement hydration. There are relatively large pores, and the structure is not compact, so the strength is relatively poor. In addition, most of the ettringite produced by early hydration reactions is wrapped in unreacted cementitious materials, which also delays the progress of early hydration reactions (Figures 13 and 14).

After 28 days of hydration reaction, the production of hydration products in both the O-S-C and Mix-EXP was significantly improved, and the structure developed more densely. However, thanks to the aggregate effect of the volcanic ash reaction in fly ash, as the hydration reaction progresses, the hydration products will be concentrated around the fly ash sphere, which has a certain improvement in the overall strength of the cement system. At the same time, PVA fibers in the system can improve the damage resistance characteristics of cement-based materials. The fibers added to the cement system are interlaced on the network of existing hydration products such as ettringite, making the hydration products more tightly bound and improving the compactness of the material system, thereby improving the mechanical properties of the composite material.

Based on the comprehensive scanning electron microscopy imaging results, it can be concluded that the dispersion characteristics of fly ash have an improvement effect on the redistribution of cement hydration products. On this basis, adding an appropriate amount of water-reducing agent can disperse overly concentrated hydration products, optimizing the interfacial properties of cement.

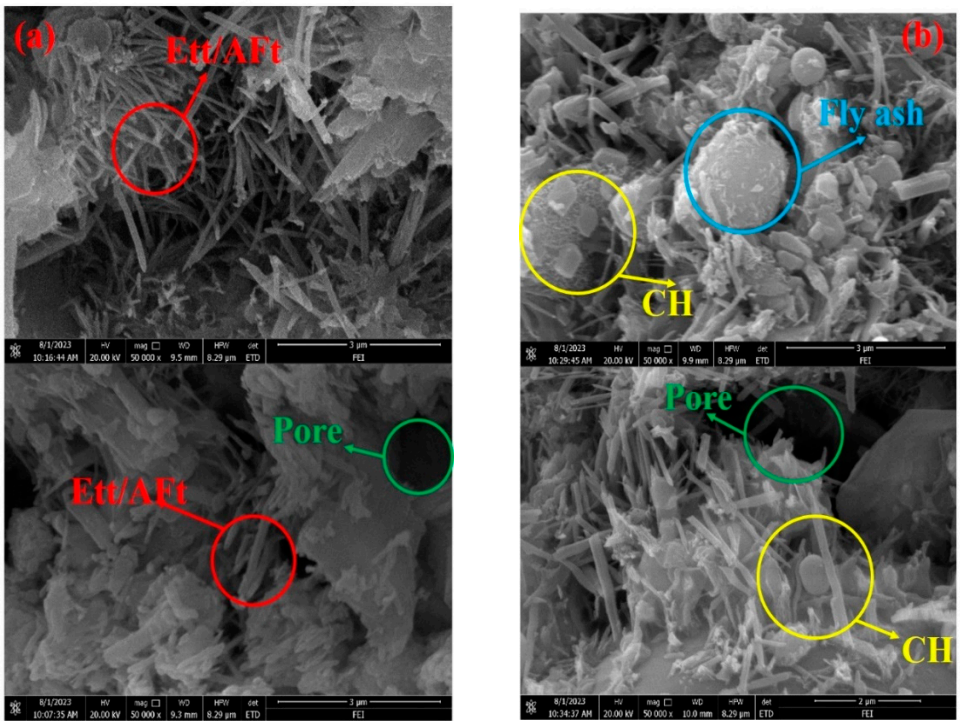

Figure 13. SEM micrograph of blank composite cement sample and experimental sample at 1 d (**a**) O-S-C (control); (**b**) Mix-EXP.

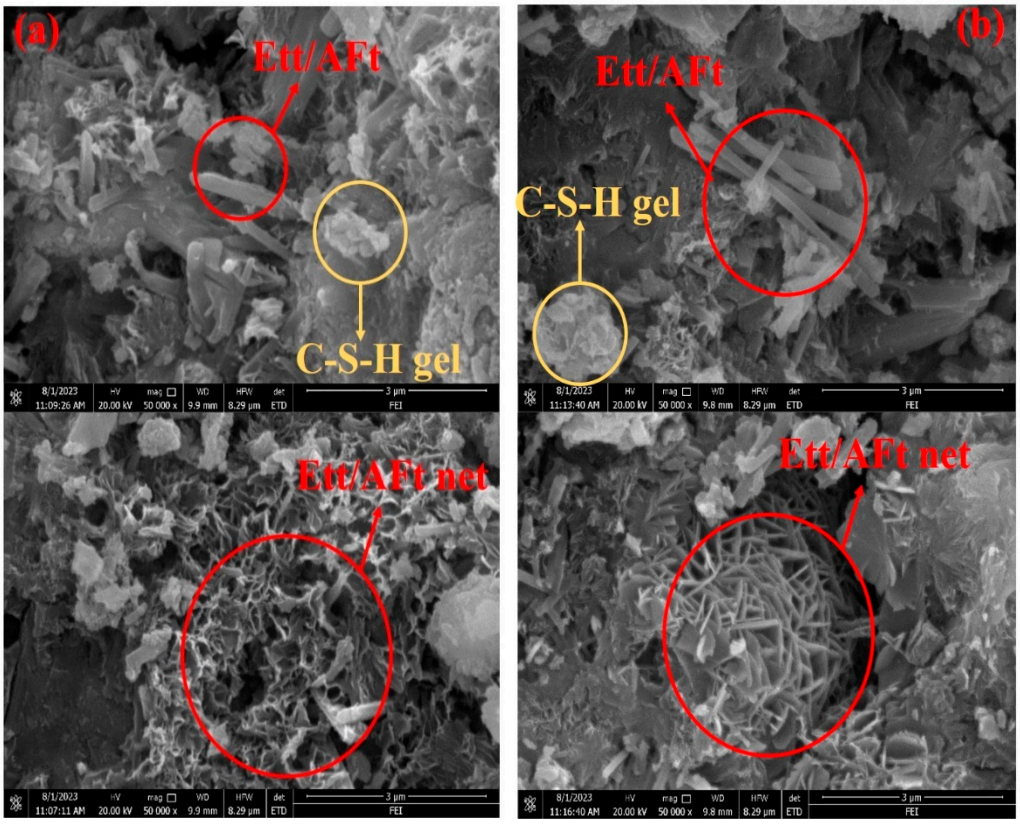

Figure 14. SEM micrograph of blank composite cement sample and experimental sample at 28 d: (**a**) O-S-C (control); (**b**) Mix-EXP.

4. Conclusions

This paper investigated the effects of fly ash and polypropylene polyvinyl alcohol mixed fibers on the structural, mechanical properties, and microstructure of a silicate sulfoaluminate composite cement system. Experiments have shown that fly ash has a crucial impact on the improvement in the strength of composite cement systems and the development of hydration. Based on the above experimental results, the following conclusions can be drawn:

(1) Adding fly ash to the composite cement system can improve the fluidity of the cement system. Although it will prolong the setting time, the content of hydration products such as ettringite and calcium hydroxide will increase in the later hydration stage due to the volcanic ash reaction. The X-RD analysis results show that although adding fly ash will affect the yield of hydration products, it will not impact the type of hydration products.

(2) The addition of PVA fibers can effectively improve the strength performance of the cement system. Compared with experimental group 7 and the blank control group (experimental group 1), the compressive strength reached 24.61 MPa after 28 days of curing, which was 13.8% higher than the control group.

(3) Adding fly ash to the composite cement system may prolong the early setting time of the cement, but it can, to some extent, improve the cement system's fluidity and positively impact the later strength. After 28 days of curing, the compressive strength of experimental group 9 reached 30.21 MPa, which increased by 70.5% compared to the group at 7 days.

(4) Adding water reducer to the cement system can significantly improve the flowability of the system with minimal impact on setting performance. Meanwhile, water reducer can make the distribution of cement hydration products more uniform, slightly improving the compressive strength of cement in the later stage of hydration.

(5) The results of the SEM scanning electron microscopy analysis showed that fly ash and water reducer played a dispersing role in the early development of the cement system. At the age of 1 day, the distribution of hydration products such as ettringite in experimental group 9 was not as concentrated as the blank control group, which may be the reason for the poor early strength of experimental group 9. After 28 days of hydration reaction, thanks to the aggregate effect of the added fly ash, as the hydration reaction progresses, the hydration products will be concentrated around the fly ash sphere, which has a specific improvement in the overall strength of the cement system. At the same time, the PVA fibers in the system can improve the damage characteristics of cement-based materials and, to some extent, enhance the compressive performance of the cement system.

Compared with traditional cement materials, the composite cement-based material obtained in this study has better mechanical and durability properties, while also considering setting time and flowability. Due to the use of fly ash and sulfoaluminate cement, the carbon emissions during the material production process are further reduced, making it more environmentally friendly. In future engineering practice, this material can be used for drilling and sealing in the mining process to improve gas extraction efficiency. It can also be used for reinforcement and repair projects in geotechnical engineering, but specific adjustments to the material formula need to be made based on construction conditions. In future research, researchers may consider using more organic materials or smaller nano additives to modify cement materials for better workability.

Author Contributions: S.W.: Funding acquisition, Resources, and Writing—review and editing. X.Z.: Conceptualization, Methodology, and Writing—original draft. J.B.: Writing—original draft. F.R.: Resources. W.L.: Supervision and Resources. S.X.: Data curation and Validation. All authors have read and agreed to the published version of the manuscript.

Funding: This paper was supported by the Guizhou Provincial Program on Commercialization of Scientific and Technological Achievements (No. [2023] general 108).

Institutional Review Board Statement: Not applicable.

Informed Consent Statement: Not applicable.

Data Availability Statement: Data is contained within the article.

Conflicts of Interest: Jiming Bao and Feng Ren are employed by Guizhou Zisenyuan Group Investment Co., Ltd. and Weidong Luo is employed by Guizhou Panjiang Coal Power Group Technology Research Institute Co., Ltd. The authors declare that they have no known competing financial interests or personal relationships that could have appeared to influence the work reported in this paper.

References

1. Wang, Q.; Gao, H.; Yu, H.; Jiang, B.; Liu, B. Method for measuring rock mass characteristics and evaluating the grouting-reinforced effect based on digital drilling. *Rock Mech. Rock Eng.* **2019**, *52*, 841–851. [CrossRef]
2. Lu, H.; Yi, J.; Liu, Q.; Cao, A.; Wei, A.; Zhang, K. A self-dissolved grouting reinforcement method for water-rich soft rock roadway. *Bull. Eng. Geol. Environ.* **2022**, *81*, 256. [CrossRef]
3. Huang, Z.; Wu, Y.; Zhang, R.; Zhong, W.; Li, S.; Zhang, C.; Zhao, K. Experimental investigation on the grouting characteristics of fractured sandstones under different confining pressures. *Geomech. Geophys. Geo-Energy Geo-Resour.* **2022**, *8*, 201. [CrossRef]
4. Jiang, H.; Qiu, X. Performance assessment of a newly developed and highly stable grouting material for a completely weathered granite dam foundation. *Constr. Build. Mater.* **2021**, *299*, 123956. [CrossRef]
5. Li, T.; Huang, F.; Li, L.; Zhu, J.; Jiang, X.; Huang, Y. Preparation and properties of sulphoaluminate cement-based foamed concrete with high performance. *Constr. Build. Mater.* **2020**, *263*, 120945. [CrossRef]
6. Zhang, L.; Su, M.; Wang, Y. Development of the use of sulfo-and ferroaluminate cements in China. *Adv. Cem. Res.* **1999**, *11*, 15–21. [CrossRef]
7. Tan, H.; Zhang, X.; He, X.; Guo, Y.; Deng, X.; Su, Y.; Wang, Y. Utilization of lithium slag by wet-grinding process to improve the early strength of sulphoaluminate cement paste. *J. Clean. Prod.* **2018**, *205*, 536–551. [CrossRef]
8. Gartner, E. Industrially interesting approaches to "low-CO_2" cements. *Cem. Concr. Res.* **2004**, *34*, 1489–1498. [CrossRef]
9. Li, H.; Hu, Y.; Lu, J.; Zhao, W.; Liu, Y.; Luo, S.; Zhu, J. Effect of AH3-PCE Ultrafine Composites on the Properties of Sulfoaluminate Cement-Based Materials. *ACS Appl. Nano Mater.* **2023**, *6*, 16643–16652. [CrossRef]
10. Zhang, C.; Shuai, B.; Jia, S.; Lv, X.; Yang, T.; Chen, T.; Yang, Z. Plasma-functionalized graphene fiber reinforced sulphoaluminate cement-based grouting materials. *Ceram. Int.* **2021**, *47*, 15392–15399. [CrossRef]
11. Lin, R.; Yang, L.; Pan, G.; Sun, Z.; Li, J. Properties of composite cement-sodium silicate grout mixed with sulphoaluminate cement and slag powder in flowing water. *Constr. Build. Mater.* **2021**, *308*, 125040. [CrossRef]
12. Shi, C.; Yang, Y. Unveiling the Effects of Quicklime on the Properties of Sulfoaluminate Cement–Ordinary Portland Cement–Mineral Admixture Repairing Composites and Their Sulphate Resistance. *Materials* **2023**, *16*, 4026. [CrossRef] [PubMed]
13. Liang, X.; Dang, W.; Yang, G.; Zhang, Y. Environmental feasibility evaluation of cement co-production using classified domestic waste as alternative raw material and fuel: A life cycle perspective. *J. Environ. Manag.* **2023**, *326*, 116726. [CrossRef] [PubMed]
14. Lippiatt, N.; Ling, T.C.; Pan, S.Y. Towards carbon-neutral construction materials: Carbonation of cement-based materials and the future perspective. *J. Build. Eng.* **2020**, *28*, 101062. [CrossRef]
15. Teara, A.; Ing, D.S. Mechanical properties of high strength concrete that replace cement partly by using fly ash and eggshell powder. *Phys. Chem. Earth Parts A/B/C* **2020**, *120*, 102942. [CrossRef]
16. Fořt, J.; Šál, J.; Ševčík, R.; Doleželová, M.; Keppert, M.; Jerman, M.; Černý, R. Biomass fly ash as an alternative to coal fly ash in blended cements: Functional aspects. *Constr. Build. Mater.* **2021**, *271*, 121544. [CrossRef]
17. Jamora, J.B.; Gudia, S.E.L.; Go, A.W.; Giduquio, M.B.; Loretero, M.E. Potential CO_2 reduction and cost evaluation in use and transport of coal ash as cement replacement: A case in the Philippines. *Waste Manag.* **2020**, *103*, 137–145. [CrossRef] [PubMed]
18. Miller, S.A.; Myers, R.J. Environmental impacts of alternative cement binders. *Environ. Sci. Technol.* **2019**, *54*, 677–686. [CrossRef] [PubMed]
19. Lobo, C.; Cohen, M.D. Pore structure development in type K expansive cement pastes. *Cem. Concr. Res.* **1991**, *21*, 229–241. [CrossRef]
20. Calvo, J.G.; Carballosa, P.; Pedrosa, F.; Revuelta, D. Microstructural phenomena involved in the expansive performance of cement pastes based on type K expansive agent. *Cem. Concr. Res.* **2022**, *158*, 106856. [CrossRef]
21. Kirchberger, I.; Goetz-Neunhoeffer, F.; Neubauer, J. Enhancing the aluminate reaction during OPC hydration by combining increased sulfate content, triethanolamine and tartaric acid. *Cem. Concr. Res.* **2023**, *170*, 107188. [CrossRef]
22. Rakhimova, N.R.; Rakhimov, R.Z. Toward clean cement technologies: A review on alkali-activated fly-ash cements incorporated with supplementary materials. *J. Non-Cryst. Solids* **2019**, *509*, 31–41. [CrossRef]
23. Gollakota, A.R.; Volli, V.; Shu, C.M. Progressive utilisation prospects of coal fly ash: A review. *Sci. Total Environ.* **2019**, *672*, 951–989. [CrossRef] [PubMed]
24. Das, D.; Rout, P.K. A Review of Coal Fly Ash Utilization to Save the Environment. *Water Air Soil Pollut.* **2023**, *234*, 128. [CrossRef]
25. Fasihihour, N.; Abad, J.M.N.; Karimipour, A.; Mohebbi, M.R. Experimental and numerical model for mechanical properties of concrete containing fly ash: Systematic review. *Measurement* **2022**, *188*, 110547. [CrossRef]

26. Ma, B.; Liu, X.; Tan, H.; Zhang, T.; Mei, J.; Qi, H.; Zou, F. Utilization of pretreated fly ash to enhance the chloride binding capacity of cement-based material. *Constr. Build. Mater.* **2018**, *175*, 726–734. [CrossRef]
27. Liao, W.; Ma, H.; Sun, H.; Huang, Y.; Wang, Y. Potential large-volume beneficial use of low-grade fly ash in magnesia-phosphate cement based materials. *Fuel* **2017**, *209*, 490–497. [CrossRef]
28. Mitchell, D.R.G.; Hinczak, I.; Day, R.A. Interaction of silica fume with calcium hydroxide solutions and hydrated cement pastes. *Cem. Concr. Res.* **1998**, *28*, 1571–1584. [CrossRef]
29. Hua, T.; Tang, J.; Zhu, J.; Tang, H.; Liu, J. Evolution of the early compressive strength of cement-slag pastes with CaO-based expansive agent. *Mater. Struct.* **2022**, *55*, 63. [CrossRef]
30. Xu, S.; Mu, F.; Wang, J.; Li, W. Experimental study on the interfacial bonding behaviors between sprayed UHTCC and concrete substrate. *Constr. Build. Mater.* **2019**, *195*, 638–649. [CrossRef]
31. Ding, Z.; Wen, J.; Li, X.; Fu, J.; Ji, X. Mechanical behaviour of polyvinyl alcohol-engineered cementitious composites (PVA-ECC) tunnel linings subjected to vertical load. *Tunn. Undergr. Space Technol.* **2020**, *95*, 103151. [CrossRef]
32. Wang, Q.; Yi, Y.; Ma, G.; Luo, H. Hybrid effects of steel fibers, basalt fibers and calcium sulfate on mechanical performance of PVA-ECC containing high-volume fly ash. *Cem. Concr. Compos.* **2019**, *97*, 357–368. [CrossRef]
33. Ji, Y.; Zou, Y.; Wan, X.; Li, W. Mechanical Investigation on Fiber-Doped Cementitious Materials. *Polymers* **2022**, *14*, 1663. [CrossRef] [PubMed]
34. Ding, C.; Guo, L.; Chen, B. An optimum polyvinyl alcohol fiber length for reinforced high ductility cementitious composites based on theoretical and experimental analyses. *Constr. Build. Mater.* **2020**, *259*, 119824. [CrossRef]
35. Deng, F.; Cao, C.; Xu, L.; Chi, Y. Interfacial bond characteristics of polypropylene fiber in steel/polypropylene blended fiber reinforced cementitious composite. *Constr. Build. Mater.* **2022**, *341*, 127897. [CrossRef]
36. Jia, E.; Mou, H.; Liu, Z.; Wang, J.; Zeng, L.; Yang, X.; Liu, P. Surface hydrophilic modification of polypropylene fibers and their application in fiber-reinforced cement-based materials. *J. Macromol. Sci. Part B* **2020**, *60*, 286–298. [CrossRef]
37. *GB/T 1346-2011*; Test Methods for Water Requirement of Normal Consistency, Setting Time and Soundness of the Portland Cement. China National Standardization Administration: Beijing, China, 2011.
38. *GB/T 2419-2005*; Test Method for Fluidity of Cement Mortar. China National Standardization Administration: Beijing, China, 2005.
39. *GB/T 17671-2021*; Test Method of Cement Mortar Strength (ISO Method). National Standardization Administration: Beijing, China, 2021.
40. Snellings, R.; Salze, A.; Scrivener, K.L. Use of X-ray diffraction to quantify amorphous supplementary cementitious materials in anhydrous and hydrated blended cements. *Cem. Concr. Res.* **2014**, *64*, 89–98. [CrossRef]
41. Hurley, R.C.; Pagan, D.C.; Herbold, E.B.; Zhai, C. Examining the micromechanics of cementitious composites using In-Situ X-ray measurements. *Int. J. Solids Struct.* **2023**, *267*, 112162. [CrossRef]
42. Aodkeng, S.; Sinthupinyo, S.; Chamnankid, B.; Hanpongpun, W.; Chaipanich, A. Effect of carbon nanotubes/clay hybrid composite on mechanical properties, hydration heat and thermal analysis of cement-based materials. *Constr. Build. Mater.* **2022**, *320*, 126212. [CrossRef]
43. Chaipanich, A.; Wianglor, K.; Piyaworapaiboon, M.; Sinthupinyo, S. Thermogravimetric analysis and microstructure of alkali-activated metakaolin cement pastes. *J. Therm. Anal. Calorim.* **2019**, *138*, 1965–1970. [CrossRef]
44. Wu, T.; Chi, M.; Huang, R. Characteristics of CFBC fly ash and properties of cement-based composites with CFBC fly ash and coal-fired fly ash. *Constr. Build. Mater.* **2014**, *66*, 172–180. [CrossRef]
45. Wang, X.; Yuan, J.; Wei, P.; Zhu, M. Effects of fly ash microspheres on sulfate erosion resistance and chlorion penetration resistance in concrete. *J. Therm. Anal. Calorim.* **2020**, *139*, 3395–3403. [CrossRef]
46. He, P.; Drissi, S.; Hu, X.; Liu, J.; Shi, C. Investigation on the influential mechanism of FA and GGBS on the properties of CO_2-cured cement paste. *Cem. Concr. Compos.* **2023**, *142*, 105186. [CrossRef]
47. Legrand, C.; Wirquin, E. Study of the strength of very young concrete as a function of the amount of hydrates formed—Influence of superplasticizer. *Mater. Struct.* **1994**, *27*, 106–109. [CrossRef]
48. Sharma, P.; Tyagi, D.; Agarwal, S.K. Effect of blended fly ash and superplasticizer on pozzolanic activity and compressive strength of cement paste. *Concr. Res. Lett.* **2011**, *2*, 336–345.
49. Stuart, K.D.; Anderson, D.A.; Cady, P.D. Compressive strength studies on portland cement mortars containing fly ash and superplasticizer. *Cem. Concr. Res.* **1980**, *10*, 823–832. [CrossRef]
50. Wang, T.; Ishida, T. Multiphase pozzolanic reaction model of low-calcium fly ash in cement systems. *Cem. Concr. Res.* **2019**, *122*, 274–287. [CrossRef]
51. Marsh, B.K.; Day, R.L. Pozzolanic and cementitious reactions of fly ash in blended cement pastes. *Cem. Concr. Res.* **1988**, *18*, 301–310. [CrossRef]
52. Luxán, M.D.; De Rojas, M.S.; Frías, M. Investigations on the fly ash-calcium hydroxide reactions. *Cem. Concr. Res.* **1989**, *19*, 69–80. [CrossRef]